A PROCEDURE TO FIND THERMODYNAMIC EQUILIBRIUM CONSTANTS FOR CO_2 AND CH_4 ADSORPTION ON ACTIVATED CARBON

T.T. Trinh[1], T. S. van Erp[1], D. Bedeaux[1], S. Kjelstrup[1,2,*], and C. A. Grande[3]

[1] Department of Chemistry, Norwegian University of Science and Technology, Trondheim, Norway
[2] Department of Process and Energy Laboratory, Delft University of Technology, Delft, The Netherlands
[3] SINTEF Materials and Chemistry, PO Box 124 Blindern, Oslo N0314, Norway

* Corresponding author: Signe Kjelstrup signe.kjelstrup@ntnu.no

ABSTRACT

Thermodynamic equilibrium for adsorption means that the chemical potential of gas and adsorbed phase are equal. A precise knowledge of the chemical potential is, however, often lacking, because the activity coefficient of the adsorbate is not known. Adsorption isotherms are therefore commonly fitted to ideal models such as the Langmuir, Sips or Henry models. We propose here a new procedure to find the activity coefficient and the equilibrium constant for adsorption which uses the thermodynamic factor. Instead of fitting the data to a model, we calculate the thermodynamic factor and use this to find first the activity coefficient. We show, using published molecular simulation data, how this procedure gives the thermodynamic equilibrium constant and enthalpies of adsorption for CO_2(g) on graphite. We also use published experimental data to find similar thermodynamic properties of CO_2(g) and of CH_4(g) adsorbed on activated carbon. The procedure gives a higher accuracy in the determination of enthalpies of adsorption than ideal models do.

1. INTRODUCTION

Equilibrium isotherms play a central role in the handling of experimental and computational data related to gas separation by adsorption processes. Cheap and efficient materials to capture and separate CO_2 are central issues in this context, and activated carbon is a promising low-cost material for CO_2 adsorption and separation.[1-4] It is common to use the ideal Langmuir theory, or variations of this theory (*e.g.* Sips, multi-site Langmuir, Toth) to describe adsorption, say, of CO_2 on activated carbon[5-7]. But one set of experimental data can be fitted to several isotherm models with the same good accuracy.[1-3, 8-16] Each model will, however, be characterized by parameters from the fit, possibly resulting in different values for the enthalpy of adsorption, ΔH . For example Schell *et al*. reported large variations in ΔH , depending on the method used, in their study of CO_2 adsorption on activated carbon type AP3-60 (Chemviron, Germany).[11] The enthalpy of adsorption from the experiments was -13.1 kJ/mol, but it was -9.1 kJ/mol from Langmuir and Sips models.

Grande *et al*. employed multi-site Langmuir, virial- and Sips models to describe isotherms for CO_2 or CH_4 on activated carbon type Maxorb (Kansai Coke and Chemicals, Japan) at high pressures.[2] The authors reported that the different models yielded enthalpies of adsorption ranging from -19.7 to -23.8 kJ/mol for CO_2, and -16.4 to -17.1 kJ/mol for CH_4.

Computer simulations have now become powerful tools in the study of adsorption of gases on porous activated carbon.[17-23] Grand Canonical Monte Carlo (GCMC) and molecular dynamics (MD) simulations are routinely used to obtain adsorption enthalpies and activity coefficients of adsorbed components.[24, 25] The two methods mentioned produce the same results, and they do also agree with a new simulation method, the small system method.[26] A comparison of computational methods is not in the scope of this work. Rather we shall use existing isotherm data, including experimental data, to develop a new data reduction procedure.

Most data, whether they are obtained from GCMC or MC simulations or experiments, fit very well with the Langmuir theory. A relatively good fitting quality may nevertheless be not representative for the actual physical events. Knowledge of activities and activity coefficients are essential for a precise description of adsorbed states. The state is frequently non-ideal[27-29] and a major obstacle is then to find the activity coefficient. The aim of this paper is to offer a new procedure to obtain such knowledge. To the best of our knowledge, the thermodynamic equilibrium constant was not considered before in the context of computer simulations; its use was mainly limited to describe experimental data.[27, 28] We shall demonstrate how we can take advantage of the thermodynamic factor to find the activity coefficient and the thermodynamic equilibrium constant from literature data. This route to central thermodynamic properties has so far been little explored from this basis, and we shall see that it offers high precision in the processed data. As examples for illustration of the method, we shall take recent results from MD simulations of CO_2 on graphite (using the small system method), and experimental results for CO_2 and CH_4 on an activated carbon.

The paper is structured as follows. We give first the well-known thermodynamic relations for interpretation of adsorption equilibrium, and the procedure for data evaluation based on the thermodynamic factor. The method is next applied to data available in literature for adsorption of CO_2 on two layers of graphite.[30, 31] The equilibrium between the first and second gas layers on graphite and the gas, give data that will be fitted to the Langmuir or Henry laws and characterized by the (same) chemical potential. The heats of adsorption from the different techniques will be calculated and compared with experimental data for CO_2 and CH_4 adsorption on activated carbon.[2] After the discussion, we summarize the important findings and conclude the paper.

2. THERMODYNAMIC RELATIONS

A description of CO_2 adsorption on graphite is relevant to studies of graphitic membrane separators[32]. The adsorption of a single gas, taking CO_2 as example; can be written

$$CO_2(g) + \text{graphite} \rightleftharpoons CO_2(s) \qquad (1)$$

Molecular simulations have shown that two layers (1 and 2) are formed on a graphite surface[31] for the pressures (< 350 bar) and in the temperature range (350 – 500 K) studied here. Multilayers of CO_2 have been observed on carbon materials, but such layers have not been seen under the present conditions. Two layers develop, not in sequence, but in parallel, meaning that two equilibrium conditions are relevant:

$$\text{Adsorbed layer 1} \rightleftharpoons \text{Adsorbed layer 2} \rightleftharpoons \text{gas phase} \qquad (2)$$

The two layers are in equilibrium with each other and with the gas. We may also deal with the two layers combined. Following Gibbs, the adsorption is defined as a surface excess concentration.[33] For layer *i* the adsorption is constructed after choosing a dividing surface. For data from molecular dynamics simulations it is convenient to choose the position indicated by β in Fig. 1. The excess total concentration is then:

$$C^s = \int_0^{\beta} C(z)dz = C_1^s + C_2^s = \int_0^{\alpha} C(z)dz + \int_{\alpha}^{\beta} C(z)dz \qquad (3)$$

where *C(z)* is the concentration (in no. of molecules /(nm)^3) and C^s is the adsorption (in no. of molecules/(nm)^2). Position β is defined when concentration of CO_2 reaches the bulk value. The excess is obtained as an excess of the graphite concentration, which here is zero. The figure gives the location with an accuracy of 5-10%, as determined by the accuracy of the gas density. There are two layers of CO_2 adsorbed on the graphite surface in Fig. 1. We refer to the integral in equation (3) from the first peak as the first layer, while the corresponding integral related to the second peak, is called the second layer with respect to the graphite surface. The total adsorption in Eq. (3) has contributions from the first and second layer, i.e. from the regions [0,α] and [α,β] (See Fig. 1). See ref [31] for more computational details.

For experimental data, it is common to speak of the total adsorption, obtained for instance from measures of weight increases. In the present case, the total adsorption will correspond to the excess surface concentration.

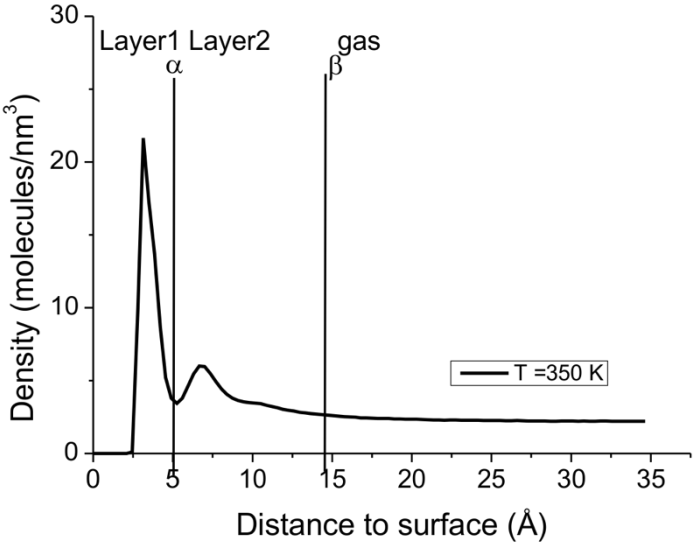

Figure 1. Density profile of CO_2 as a function of distance to the graphite surface at temperature 350 K and pressure 60 bar. We distinguish between three zones, from 0-α: first adsorbed layer (layer 1), α-β: second adsorbed layer (layer 2), and above β: gas phase.

The chemical potential for a gas adsorbed on a surface in layer i = 1,2 is defined as:

$$\mu_i^s = \mu_i^{s,0} + RT \ln a_i^s = \mu_i^{s,0} + RT \ln \gamma_i^s \frac{C_i^s}{C_i^{s,0}} \qquad (4)$$

Superscript s denotes the adsorbed phase, and a^s is the (dimensionless) activity of the adsorbed phase defined by the ratio $\gamma^s C^s / C^{s,0}$, where γ^s is the activity coefficient and $C^{s,0}$ is the concentration at full surface coverage. The standard chemical potential $\mu^{s,0}$ is commonly chosen as the chemical potential of the hypothetical ideal state at the concentration $C^{s,0}$. This hypothetical ideal state behaves according to Henry's law and has $\gamma^s = 1$ at any concentration[33]. In reality, $\mu^s(C^{s,0}) \neq \mu^{s,0}$, and the activity coefficient $\gamma^s \neq 1$, also at concentration $C^{s,0}$ and at smaller concentrations. Only in the limit $C^s \to 0$, where CO_2 particle interactions vanish, will the activity coefficient γ approache unity.[31] For the gas phase (superscript g) we have:

$$\mu^g = \mu^{g,0} + RT \ln a^g = \mu^{g,0} + RT \ln \frac{\phi P}{P^0} \qquad (5)$$

Here P and P^0 are the pressure and standard pressure of the gas, and ϕ is the fugacity coefficient. In the low pressure range, the fugacity coefficient is unity.

The activity coefficient of the adsorbed phase is of interest. A possible route, not much used, is to first find the thermodynamic correction factor, or simply, the thermodynamic factor, Γ^s.[33] At constant temperature T and surface area A, Γ^s is defined by

$$\Gamma^s = 1 + \left(\frac{\partial \ln \gamma^s}{\partial \ln C^s} \right)_{T,A}$$

The thermodynamic factor, like the activity coefficient, can in some ideal cases be understood from statistical mechanical models of adsorption, see Appendix A. The activity coefficient can be obtained by integration from zero adsorption ($C^s \to 0 : \gamma^s = 1$) to the actual state, see ref [31] for more details:

$$\int_0^{\ln \gamma^s} d \ln \gamma^s = \int_{-\infty}^{\ln C^s} (\Gamma^s - 1)\, d \ln \mathrm{C}^s \qquad (6)$$

Results for Γ^s and γ^s for pure CO_2 on a graphite surface were published previously[31] using a relatively newly developed method, the so-called Small System Method to find the thermodynamic factor.[31, 34] In this computational method, particle fluctuations were sampled according to:

$$\frac{1}{\Gamma} = \left[\frac{\langle N^2 \rangle - \langle N \rangle^2}{\langle N \rangle} \right]_{T,A} \qquad (7)$$

Here N denotes the particle number in the sampling volume and the brackets denote that the average is taken. Expression (7) obeys a finite-size effect, which was exploited to obtain the thermodynamic factor as function of A.[35, 36] The temperature and pressure were controlled, the sampling disk area, A, was varied, and Γ^s was obtained by extrapolation to an infinitely large area.

When the fugacity coefficient of the gas is constant, the thermodynamic factor can also be expressed by:[21, 24]

$$\frac{1}{\Gamma^s} = d \ln C_i^s / d \ln P = \frac{P}{C_i^s} \frac{dC_i^s}{dP} \qquad (8)$$

Experimental data needed to obtain Γ^s from this formula are available for CO_2 or CH_4 on activated carbon.[2] We shall see how also these data can be used to give accurate thermodynamic data for the adsorbed phase.

The equilibrium condition for multilayer adsorption CO_2 on a graphite surface is:

$$\mu_1^s = \mu_2^s = \mu^s = \mu^g \qquad (9)$$

For layers 1 and 2, we have:

$$\mu_1^{s,0} + RT \ln \gamma_1^s \frac{C_1^s}{C_1^{s,0}} = \mu_2^{s,0} + RT \ln \gamma_2^s \frac{C_2^s}{C_2^{s,0}} \qquad (10)$$

$$\mu_1^{s,0} - \mu_2^{s,0} = -RT \ln \left(\frac{\gamma_1^s}{\gamma_2^s} \frac{C_1^s}{C_2^s} \frac{C_2^{s,0}}{C_1^{s,0}} \right) \qquad (11)$$

We choose for convenience $C_1^{s,0} = C_2^{s,0}$, giving the equilibrium constant for equilibrium between layers 1 and 2 equal to:

$$K_{1,2}^{a} = \frac{\gamma_1^s}{\gamma_2^s}\frac{C_1^s}{C_2^s} \qquad (12)$$

Similarly, for equilibrium between adsorbed CO_2 and gas phase, we have for each layer, and for the total layer that

$$\mu^{g,0} - \mu_i^{s,0} = -RT\ln\left(\frac{1}{\gamma_i^s}\frac{P}{C_i^s}\frac{C_i^{s,0}}{P^0}\right) \quad i=1, 2, \text{total} \qquad (13)$$

The equilibrium constant for equilibrium between an adsorbed layer and an ideal gas phase then becomes:

$$K_{i,g}^{a} = \frac{\gamma_i^s C_i^s}{P} \qquad (14)$$

This equilibrium constant $K_{i,g}^{a}$ is, to the best of our knowledge, not in active use for data reduction. In the most common route, one assumes that the adsorbed state follows e.g Henry's law or a Langmuir type isotherm. Henry's law sets $\gamma_i^s = 1$ for low concentrations or small enthalpies of adsorption, and gives

$$K_{i,g}^{H} = \frac{C_i^s}{P} \qquad (15)$$

In the ideal Langmuir isotherm, there is always a single layer of adsorption. The degree of adsorption is measured by the fractional coverage $\theta_i = \frac{C_i^s}{C_i^{s,\max}}$ where $C_i^{s,\max}$ is the maximum adsorption. This leads to

$$K_{i,g}^{L} = \frac{\theta}{1-\theta}\frac{P^0}{P} \qquad (16)$$

Using $P^0 = 1\text{bar}$ and $\tilde{P} = P/P^0$, the Langmuir constant is obtained by fitting experimental data to the functional form of the isotherm:

$$\frac{C^s}{C^{s,\max}} = \frac{K_{i,g}^{L}\tilde{P}}{1+K_{i,g}^{L}\tilde{P}} \qquad (17)$$

The temperature variation in K has been used to find the enthalpy of adsorption ΔH from van't Hoff's equation

$$K = K^0 \exp(-\frac{\Delta H}{RT}) \qquad (18)$$

By introducing equations (15) and (17) into equation (8) we obtain the inverse thermodynamic correction factor for the Henry and Langmuir adsorption isotherms as:

$$\frac{1}{\Gamma^s_{Henry}} = 1 \text{ and } \frac{1}{\Gamma^s_{Lanmguir}} = 1 - \frac{C^s}{C^{s,\max}} \qquad (19)$$

The statistical mechanical model in Appendix A, relates these expressions to an ideal value of the adsorption energy, E_{ads}, which in good approximation becomes equal to minus the enthalpy of adsorption.

We show below that an isotherm for CO_2 gas adsorbed on a graphite surface, obtained from molecular dynamics simulations, can be fitted to Langmuir and Henry models with good accuracy. However, these ideal models lead in these cases to enthalpies of adsorption which differ from the value calculated from the van't Hoff equation and equilibrium data. We will show that inclusion of non-ideal terms in an earlier phase can mend this situation and yield more accurate data. We next examine experimental data for CO_2 and CH_4 on activated carbon. New plots of activities of the adsorbed gases will be presented, and equilibrium constants and enthalpies of adsorption will be determined for the two data sets.

3. RESULTS AND DISCUSSION

3.1. Thermodynamic data from computer simulations

Molecular dynamics (MD) simulations were performed earlier to study CO_2 adsorption on a graphite surface.[31] The adsorption of CO_2 was determined from equation (3). Two layers were found, cf. Figure 1. These data are now used to obtain the equilibrium constant and enthalpy of adsorption.

We first plotted the adsorption of each layer as a function of pressure. The results are shown in the Appendix B, Figures S1 and S2. The excess adsorption of the first layer was fitted very well to a Langmuir equation, while the second layer followed Henry's law (Figure S1). This agrees with a view that the first layer interacts with the graphite surface, while second layer is more gas-like. The two layers develop simultaneously, not sequentially, possibly because their adsorption energies are of the same order of magnitude. The combination of the two layers was also considered as one total layer.[31] The equilibrium between the first and the second layer was next described by the Langmuir equation (Figure S2). The total layer in equilibrium with the gas was also fitted to a Langmuir type isotherm, as has been done by many authors.[1-3, 9, 12, 13, 37, 38] The curves fitted

to the Langmuir and Henry laws had all a regression coefficient $R^2 > 0.98$. The Langmuir and Henry constants obtained from the fits, are presented in Table 1.

Table 1. Langmuir and Henry constants for various equilibria obtained by fitting data for CO_2 adsorption on a graphite surface to the isotherms. The subscripts indicate the layers involved in the equilibrium.

T (K)	$K^L_{1,g}$	$K^H_{2,g}$	$K^L_{1,2}$	$K^L_{\text{total},g}$
300	0.064	0.111	0.956	0.022
350	0.026	0.052	0.601	0.010
400	0.013	0.036	0.387	0.006
450	0.008	0.024	0.275	0.004
500	0.006	0.019	0.233	0.003
550	0.004	0.015	0.166	0.002

By next using the statistical mechanical model of Appendix A, we calculated the energy of adsorption from a linear fit of the thermodynamic correction factor Γ vs pressure (eq. A13). The result for K^L obtained from Fig. S3, were in excellent agreement with the first mentioned results obtained from the Langmuir isotherm. This provides therefore a route to find the Langmuir constant via Γ of the adsorbed phase.

Equilibrium constants

We can now find the true equilibrium constant for equilibrium between the first and second layer from equation (12), and for equilibrium between each of the layers and the gas, *cf*. equation (14). The activity coefficients for the layers were taken from ref [31], and the simulation results were used to calculate the constant $K^a_{i,g}$ for i=1,2, as depicted in Figure 2 and Figure 3. The figures show that the activity constant times the surface excess concentration for one layer is linear in the corresponding product for the other layer, or in the pressure. The slopes decrease with increasing temperature. The product obtained for layer 1 increases faster than that for layer 2, because layer 1 is confined and has a stronger interaction with the graphite surface.[31] It is clear that the activity coefficients of the layers decide the behavior of the adsorbed layers, in agreement with equation (19).

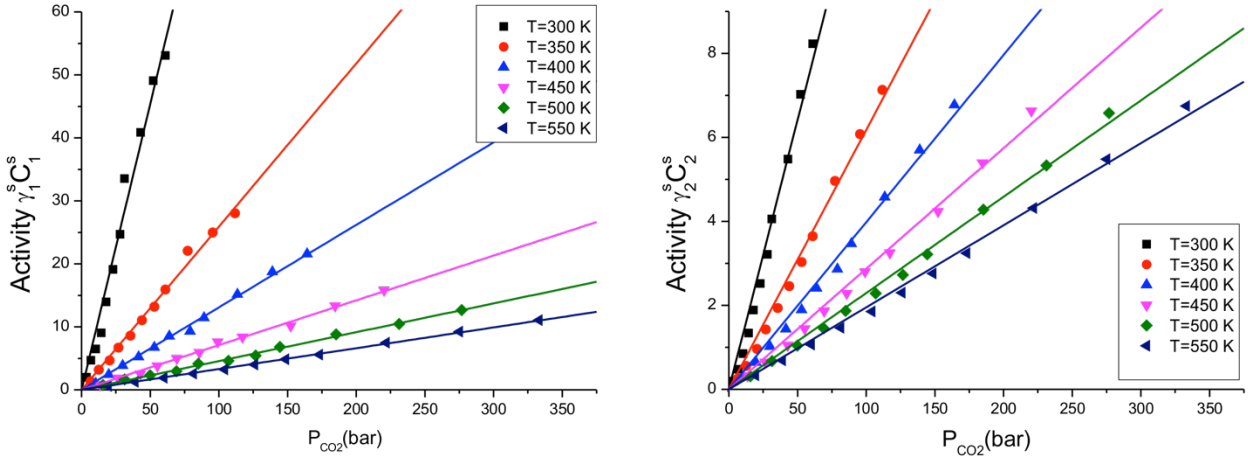

Figure 2. The dependence of the activity of the first layer (a) and second layer (b) on the CO_2 pressure. The activity coefficient was obtained from Small System Method. The slopes of the linear fit give the equilibrium constant.

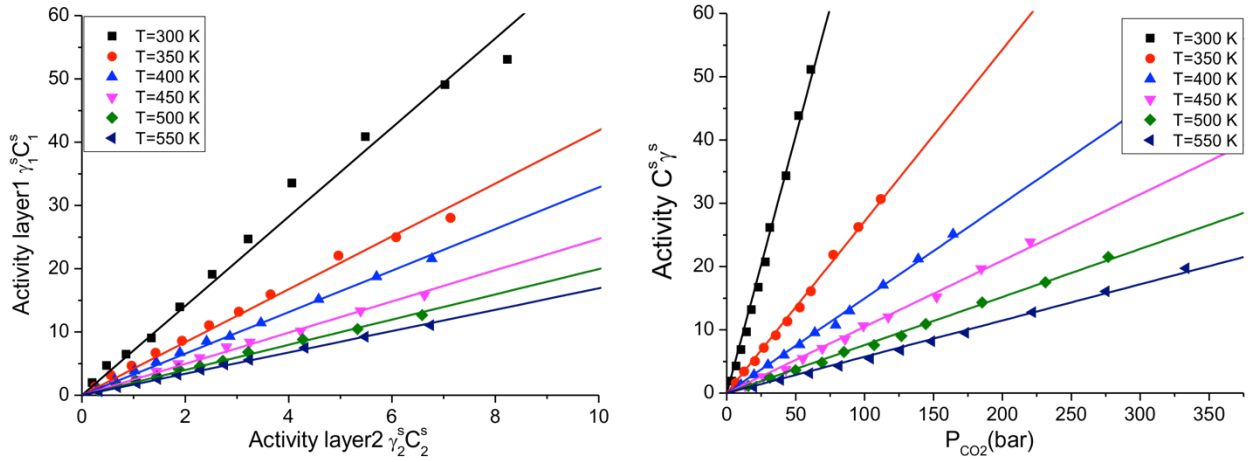

Figure 3. The dependence of the (dimensionless) activity of the first layer *vs.* that of the second layer (a) and the activity of the total layer *vs.* the CO_2 pressure. The activity coefficient was obtained from the Small System Method[25] The slopes of the linear fits give the equilibrium constant.

Table 2. Thermodynamic equilibrium constant for equilibrium between layers of CO_2 and gas at different temperature.

T (K)	$K^a_{1,g}$	$K^a_{2,g}$	$K^a_{1,2}$	$K^a_{\text{total},g}$
300	0.91	0.13	7.05	0.81
350	0.26	0.06	4.18	0.27
400	0.13	0.04	3.28	0.15
450	0.07	0.03	2.47	0.10
500	0.05	0.02	1.99	0.08
550	0.03	0.02	1.69	0.06

The linear fits of the simulation data give the thermodynamic equilibrium constants from the slopes of the lines. The results for the equilibrium constants are presented in Table 2. The data have all a regression coefficient $R^2 > 0.99$, which indicate that the method for their determination is precise.

Enthalpy of adsorption

The enthalpy of adsorption was obtained by plotting the natural logarithm of the equilibrium constant as a function of $1/T$, as shown in Figure 4. The data shows that linear fits can be obtained with either the Langmuir or the Henry constants, or with the true thermodynamic equilibrium constant for each pair of layers. From these fits, the enthalpies of adsorption were obtained using equation (18). The results are given in Table 4. Independent of the method used, we find the highest enthalpy of adsorption, by considering the equilibrium between the gas and layer 1 alone (square black points). This is reasonable, as the first layer is stronger adsorbed than the second layer (red circles), or the (average) total layer (pink down-wards pointing triangles). The equilibrium between the two surface layers (blue upwards-pointing triangles) gives the smallest enthalpy of adsorption; an incremental change from one layer to another. The enthalpy of adsorption of the total layer falls naturally between that obtained for the second and first layers alone.

We see from Table 3 that the Langmuir and Henry laws constants underestimate the enthalpy of adsorption by about 10%, compare the two last columns. The result depicted in Figure S3 of Appendix B (-12.8 kJ/mol) does the same. The enthalpy of adsorption of the total layer (-14.2 kJ/mol) is in better agreement with the experimental data from calorimetric measurements (-16.2 - -14.7 kJ/mol).[13] In general, the heat of adsorption of CO_2 in activated carbon depends strongly on the material.[2, 3, 9, 11, 12]

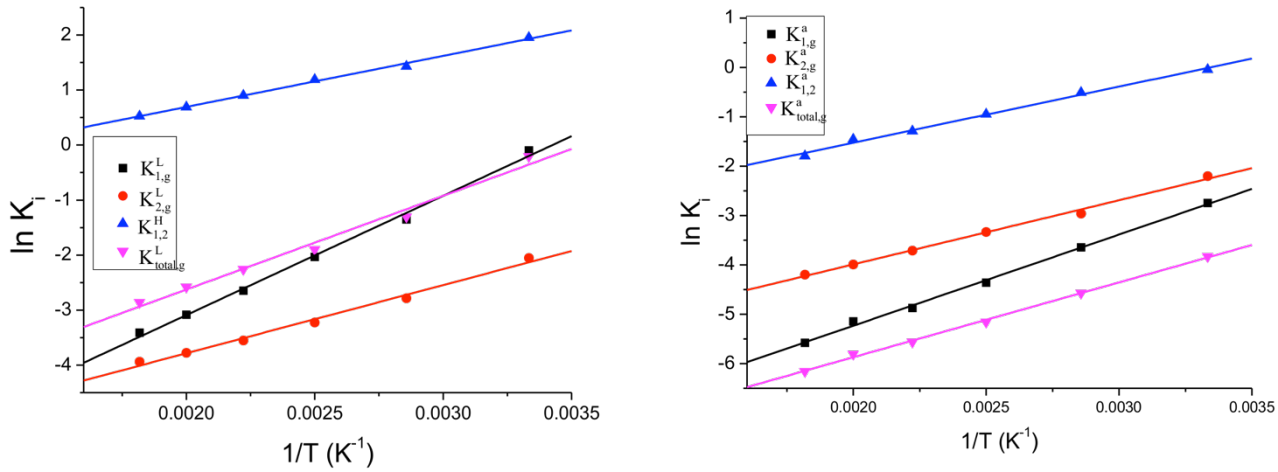

Figure 4. The natural logarithm of the Langmuir and Henry's laws' constant vs $1/T$ (a) and the equilibrium constant vs $1/T$ (b). The curves apply to CO_2 adsorption on graphite surface. The straight lines are fits to equation (18) for equilibria of different layers, as indicated by the subscript of the equilibrium constant.

Table 3. Enthalpy of adsorption (kJ/mol) between various pairs of layers.

Enthalpy of adsorption between layers (kJ/mol)	From Langmuir, Henry constants	From true equilibrium constant
Layer 1, gas $\Delta H_{1,g}$	-15.4	-18.0
Layer 2, gas $\Delta H_{2,g}$	-10.8	-10.3
Layer 1, Layer 2 $\Delta H_{1,2}$	-9.4	-7.7
Total layer, gas $\Delta H_{\text{total},g}$	-12.6	-14.2

The difference in adsorption enthalpy of layers 1 and 2 agree with the relation $\Delta H_{1,2} = \Delta H_{1,g} - \Delta H_{2,g}$, but *only when the true equilibrium constants are used*. In the Langmuir and Henry models, such a consistency is not obtained.

The thermodynamic factor

The inverse thermodynamic factors from the molecular simulations are compared with results from the numerical analysis using equation (8) in Figure 5.

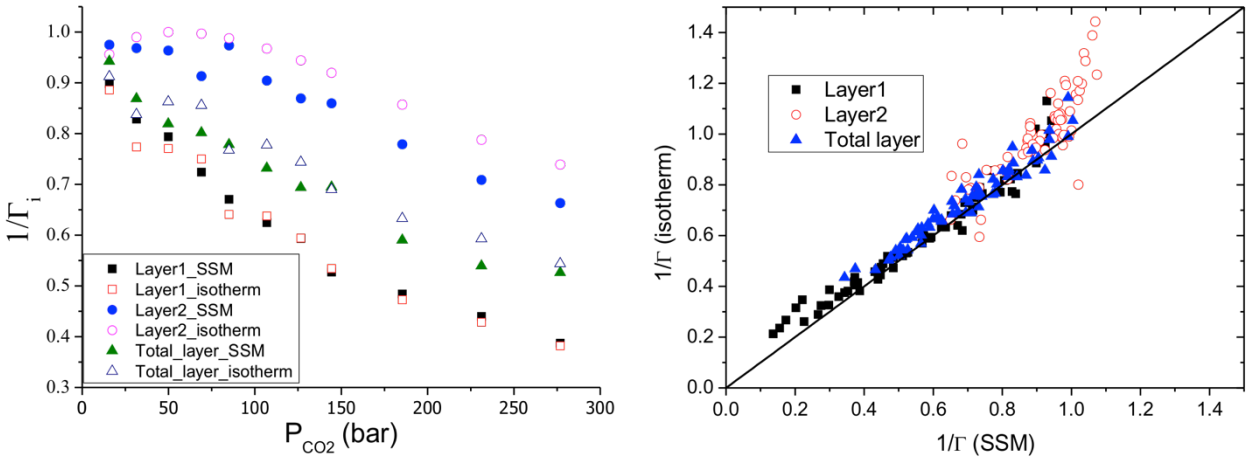

Figure 5. (a) The inverse thermodynamic factor for the different layers, as a function of pressure, obtained by the isotherm relation and the Small System Method at T = 350 K . The low pressure limit of $1/\Gamma_i$ is 1. (b) All values of $1/\Gamma$ of the two methods are shown. The scatter of data for layer 2 is due to the low density of particles in the sampling volume

The results in Figure 5 a) and b) show a good agreement between the methods at T = 350K. The deviation from unity in the slope of Figure 5 b) is most likely due to noise in the simulations at low gas densities. The low pressure limit of the inverse thermodynamic factor is unity, and we see that all curves can be drawn to approach this value (Figure 5 a). A value below unity means that repulsive forces dominate in the surface, as is to be expected, increasing with the pressure or the surface excess adsorption. Also Collell and Galliero[39] have calculated the thermodynamic factor of a Lennard-Jones system in confinement using the Small System Method, and found similar variations.

3.2. Thermodynamic data from experimental isotherms

We have seen above that the choice of isotherm model to fit experimental data is important for internal consistency in the data set. It has been shown that several models can be used to fit to one set of data, but that the sets are not always compatible with one another. [9, 11] It is therefore of interest to examine the various ways to deal with the experimental data further, taking the adsorption of CO_2 and CH_4 on an activated carbon[2] as examples. It was shown that the data set could be fitted well to multi-site Langmuir, Sips and Virial models.

We start by calculating the thermodynamic correction factor and activity coefficient from equations (8) and (6).[31] The equilibrium constant was then calculated from equation (14) leading to the enthalpy of adsorption in a similar fashion as before.

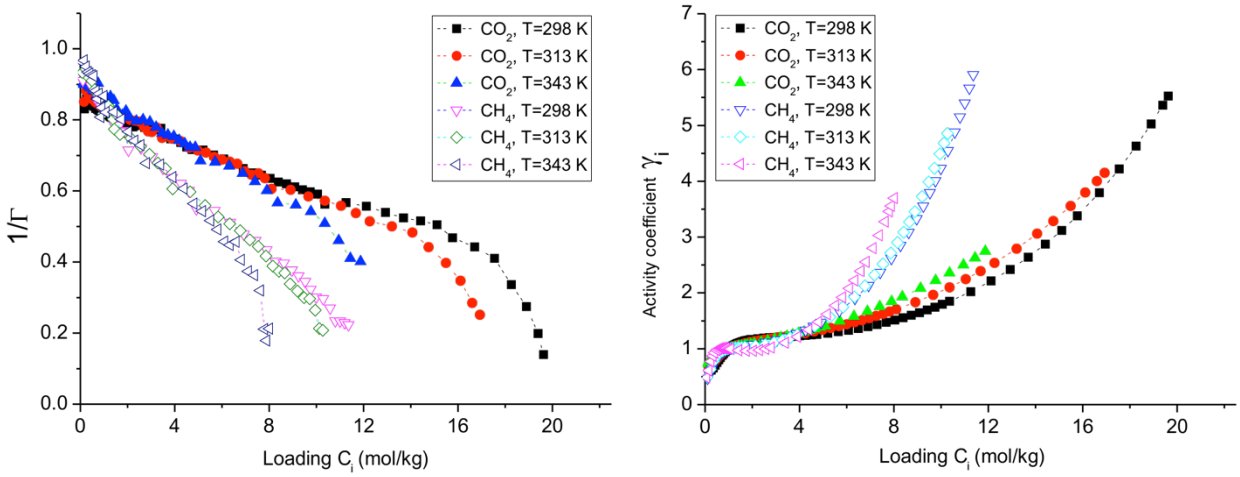

Figure 6. The inverse thermodynamic correction factor (left) from equation (8) and activity coefficient (right) from equation (6) of CO_2 and CH_4 adsorbed on activated carbon (Maxorb, The Kansai Coke and Chemicals, Japan) from the experimental data of Grande *et al.* [2]

Figure 6 presents the results for the inverse of thermodynamic correction factor $1/\Gamma_i$ and the activity coefficient γ_i of CO_2 and CH_4. Both $1/\Gamma_i$ and γ_i approach unity at low adsorptions as they should. The data show that $1/\Gamma_i$ decreases non-linearly with the excess adsorption and that the activity coefficient increases with the same. This is expected, as a decline in the inverse thermodynamic factor below 1, or, equivalently, a rise in the activity coefficient beyond 1, signals repulsive interactions in the adsorbed state at the surface. Defects in the structure of the material used may give rise to the non-linear variation in $1/\Gamma_i$. This knowledge of the limit behavior of the functions helps us avoid experiments with loadings in the difficult low density limit. The data recorded at very low densities at 343 K (Figure 6 right) may have a relatively large uncertainty due to the small loading.

We plotted the calculated value of the activity coefficient and the adsorption versus gas pressure in Figure 7. It is now remarkable that the curve is linear in most of the cases. An excellent linear fit can be obtained

($R^2 > 0.99$). The natural logarithm of the slope is also linear with the inverse temperature, providing us with the enthalpy of adsorption. A comparison between the values of enthalpies of adsorption obtained in the various scenarios is presented in Table 4.

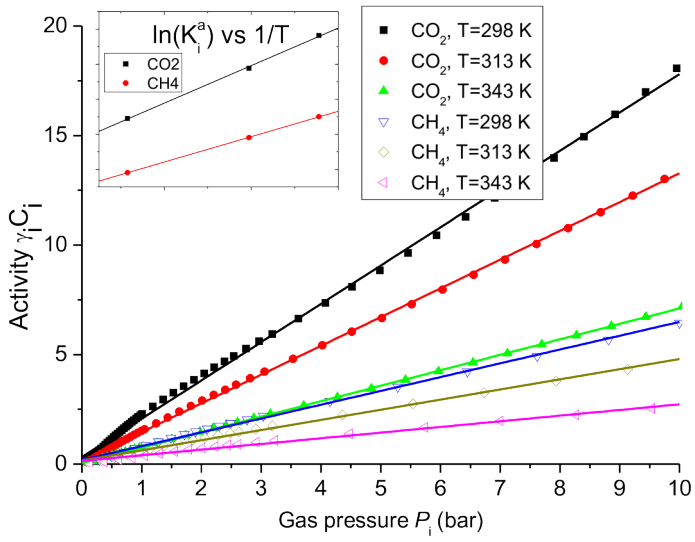

Figure 7. The linear relation between the activity of CO_2 and CH_4 adsorbed on activated carbon and pressure from experimental data of Grande *et al.*[2] The straight line is a linear fit to equation (14). The insert shows the relation between the natural logarithm of the slope and the inverse temperature for the three temperatures investigated.

Table 4. Calculated enthalpy of adsorption for CO_2 and CH_4 on an activated carbon from various thermodynamic models using the experimental data of Grande *et al.*[2]

Heat of adsorption (kJ/mol)	Activity model(this work)	Virial[2]	Multi-site Langmuir[2]	Sips[2]
CO_2	-22.3	-23.8	-21.3	-19.7
CH_4	-15.1	-17.1	-16.7	-16.4

The enthalpy of adsorption calculated from the true equilibrium constant is comparable to values from the simplified models within an error of 10% (Table 4). The advantage of using the thermodynamic equilibrium constant is that it is unique. Another benefit of this approach is to avoid unphysical fits to the Langmuir model, when the interaction adsorbate-adsorbate is comparable to the adsorbent-adsorbate interaction, see Szőri *et al.*[40] for a recent discussion

The activity of the adsorbed species is needed in order to understand the performance of the membrane in gas separation process. In the design of new membranes for gas separation purposes, this is the property to tune. The thermodynamic correction factor can furthermore be used to relate Fick diffusion coefficients and Maxwell-Stefan diffusion coefficients.

The use of empirical models in the simulation of transport, say in the break-through curve of CO_2 and CH_4 in activated carbon, gives different results.[2] To have one consistent model will be an advantage for further process modeling, say of adsorption of mixtures,[27-29] or transport in fixed-bed reactors. This will be considered in future work.

4. CONCLUSIONS

We have shown how the thermodynamic correction factor can be used with simulations or experimental data to find the surface activity coefficient of adsorbed pure components. This parameter provides a good route to thermodynamic data from the system's isotherms. We demonstrated the method for two-layer adsorption of CO_2 on a graphite surface, and for CO_2 and CH_4 on an activated carbon. Equilibrium constants and enthalpies of adsorption were determined. These results compared well with calorimetric measurements. The true thermodynamic data give precisions higher than obtainable from fits to Langmuir or Henry models. We draw the important conclusion, that instead of fitting data to system isotherms, one should rather find the thermodynamic factor, the activity coefficient and the true equilibrium constant. This could provide an initial step in a more complex target to describe multicomponent adsorption. The possibility to access the activity coefficient is important in gas separation, transport and membrane design. The method proposed here might be advantageous for accurate predictions of multicomponent adsorption equilibrium isotherms.

ACKNOWLEDGMENT

The authors acknowledge The Research Council of Norway NFR project no 209337 and The Faculty of Natural Science and Technology, Norwegian University of Science and Technology (NTNU) for financial support. The calculation power was granted by The Norwegian Metacenter for Computational Science (NOTUR).

APPENDIX A

A STATISTICAL MECHANICAL MODEL FOR THERMODYNAMIC CORRECTION FACTOR

We present a statistical mechanical model for Eq.(19). We start by writing the microscopic definition of the chemical potential.

$$\mu = k_B T \ln\left(N \frac{\int dR^{N-1} e^{-\beta U(R^{N-1})}}{\int dR^{N} e^{-\beta U(R^{N})}} \Lambda^3 \right) \tag{A1}$$

where U is the total potential energy function of the system, Λ is the thermal wave length, and R^N denotes the full set of molecular coordinate of an N particle system. The factor $\beta = 1/k_B T$ with k_B being the Boltzmann constant. Then, by inverting Eq. 5 we obtain

$$a = v^* N \frac{\int dR^{N-1} e^{-\beta U(R^{N-1})}}{\int dR^{N} e^{-\beta U(R^{N})}} \tag{A2}$$

where the dependency on μ^0 and Λ have been adsorbed into the constant $v^* = \exp(-\beta\mu^0)\Lambda^3$. For an ideal gas $U = 0$, and therefore

$$\mu = k_B T \ln\left(\frac{N\Lambda^3}{V}\right) = k_B T \ln\left(\beta P \Lambda^3\right), \quad a = v^* N / V = v^* \beta P \tag{A3}$$

where we used the ideal gas law on the form $PV = Nk_B T$. For the adsorbed layer we now consider two approximate models. The simplest model, the one obeying Henry's law, implies that adsorption is proportional to the gas pressure. The model describing this assumes that each molecule that adsorbs reduces the total energy by adsorption energy E_a irrespective of the occupancy of the surface. In other words, in the adsorption layer $U = -NE_a$ which gives

$$\mu = -E_a + k_B T \ln\left(C^s \Lambda^3\right), \quad a = v^* C^s e^{-\beta E_a} \tag{A4}$$

with $C^s = N / V$ where N and V are the number in and volume of the surface layer.

The second model is the Langmuir model where particles are adsorbed on vacancy sites that can only be singly occupied. As derived in ref 7, the chemical potential and activity of this model is given by

$$\mu = -E_a + k_B T \ln\left[\frac{\theta}{(1-\theta)}\frac{\Lambda^3}{V_{\text{vac}}}\right], a = v^* \frac{e^{-\beta E_a}}{V_{\text{vac}}}\frac{\theta}{(1-\theta)} \tag{A5}$$

where V_{vac} is the volume of the vacancy pocket. Now, since the activity $a = \gamma C^s / C^{s,0}$. with the standard state concentration $C^{s,0}$ corresponding to the concentration of maximum occupancy, we can write the activity coefficient $\gamma = a / \theta$ or for both cases:

$$\gamma = v^* C^{s,0} e^{-\beta E_a} \qquad \text{Henry} \tag{A6}$$

$$\gamma = \frac{v^* e^{-\beta E_a}}{V_{\text{vac}}(1-\theta)} \qquad \text{Langmuir}$$

Now, let us consider Γ of the adsorption layer that is in contact with a gas

$$\Gamma = \frac{\langle N \rangle}{\langle N^2 \rangle - \langle N \rangle^2} \tag{A7}$$

where the grand canonical ensemble average is defined as

$$\langle \ldots \rangle = \frac{\sum_{N=0}^{\infty} \int \ldots \rho(R^N) dR^N}{\sum_{N=0}^{\infty} \int \rho(R^N) dR^N} \tag{A8}$$

with the probability distribution $\rho(R^N) \propto e^{-\beta W(R^N)} e^{\beta\mu N} / N! \propto e^{-\beta W(R^N)} (\beta P)^N / N!$. This implies for the Henry

model that

$$\langle N\rangle = \frac{\sum_N N(Ve^{\beta E_{ads}}\beta P)^N / N!}{\sum_N (Ve^{\beta E_{ads}}\beta P)^N / N!} = Ve^{\beta E_{ads}}\beta P \qquad \text{(A9)}$$

$$\langle N^2\rangle = \frac{\sum_N N^2(Ve^{\beta E_{ads}}\beta P)^N / N!}{\sum_N (Ve^{\beta E_{ads}}\beta P)^N / N!} = Ve^{\beta E_{ads}}\beta P(Ve^{\beta E_{ads}}\beta P+1)$$

Where we used $\sum_N x^N / N! = \exp(x)$, $\sum_N Nx^N / N! = x\exp(x)$, and $\sum_N N^2x^N / N! = x(x+1)\exp(x)$. We used P for the gas pressure while V and N are properties of the adsorption layer. By introducing these expressions into the relation A7 we obtain

$$\Gamma = \frac{Ve^{\beta E_{ads}}C}{Ve^{\beta E_{ads}}C(Ve^{\beta E_{ads}}C+1)-(Ve^{\beta E_{ads}}C)^2} = 1 \qquad \text{Henry} \qquad \text{(A10)}$$

This is expected from Eq. (19). For the Langmuir model, we replace the integral by $V_{vac}^N M(M-1)...(M-N+1)$ as in ref 7. Then, by using the definition of the binomial coefficients we can write

$$\langle N\rangle = \frac{\sum_N N\binom{M}{N}(V_{vac}e^{\beta E_{ads}}\beta P)^N}{\sum_N \binom{M}{N}(V_{vac}e^{\beta E_{ads}}\beta P)^N} = \frac{MV_{vac}e^{\beta E_{ads}}\beta P}{V_{vac}e^{\beta E_{ads}}\beta P+1} \qquad \text{(A11)}$$

$$\langle N^2\rangle = \frac{\sum_N N^2\binom{M}{N}(V_{vac}e^{\beta E_{ads}}\beta P)^N}{\sum_N \binom{M}{N}(V_{vac}e^{\beta E_{ads}}\beta P)^N} = \frac{MV_{vac}e^{\beta E_{ads}}\beta P(MV_{vac}e^{\beta E_{ads}}\beta P+1)}{(V_{vac}e^{\beta E_{ads}}\beta P+1)^2}$$

Here we used $\sum_N \binom{M}{N}x^N = (x+1)^M$, $\sum_N \binom{M}{N}Nx^N = Mx(x+1)^{M-1}$, and $\sum_N \binom{M}{N}N^2x^N = Mx(x+1)^{M-2}(xM+1)$

By introducing these expressions, we obtain

$$\Gamma = V_{vac}e^{\beta E_{ads}}\beta P+1 \qquad \text{Langmuir} \qquad \text{(A12)}$$

We can relate this to the Langmuir constant as $K_{i,g}^L = V_{vac}e^{\beta E_{ads}}\beta$ which gives

$$\Gamma = K_{i,g}^L P+1 \qquad \text{(A13)}$$

Finally, by substitution of the inverse Langmuir equation $P = \theta / K_{i,g}^{L}(1-\theta)$ we end up at Eq. (19).

APPENDIX B

LANGMUIR AND HENRY EQUILIBRIUM CONSTANTS FROM SIMULATION DATA

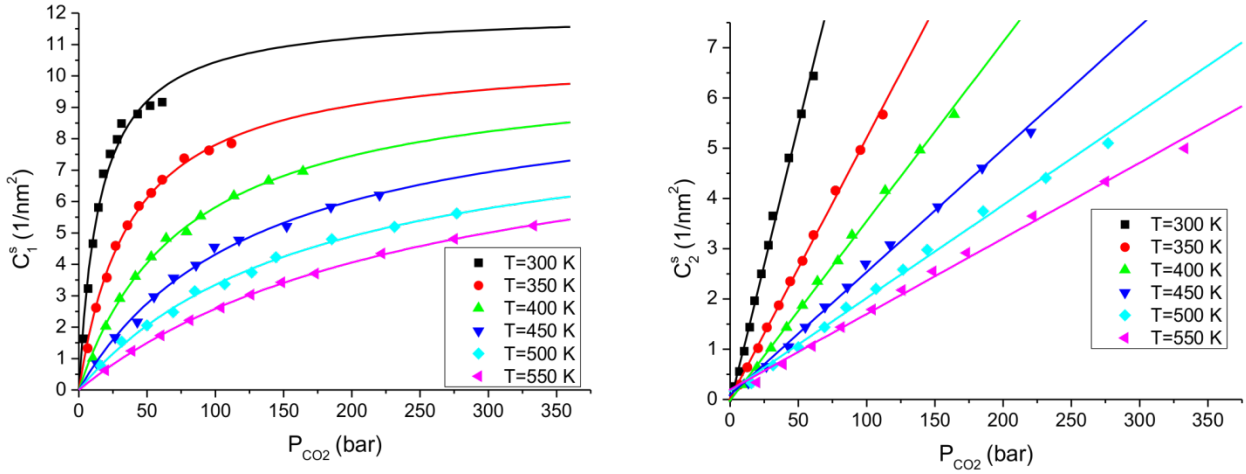

Figure S1. Adsorption isotherm of the first (a) and second layer (b) as funciton of pressure at different temperatures. The straigh lines are fitted with Langmuir (layer 1) and Henry (layer 2) isotherms.

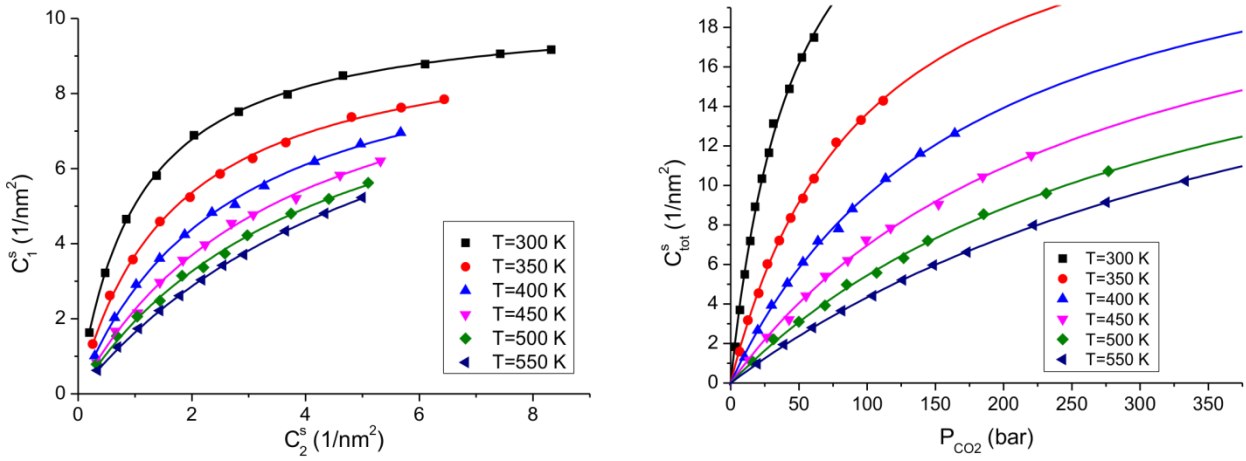

Figure S2. Adsorption isotherms valid for the first and second layers (a), and for the total layer and the gas (b) at different temperatures. The straight line is obtained from fits with a Langmuir isotherm .

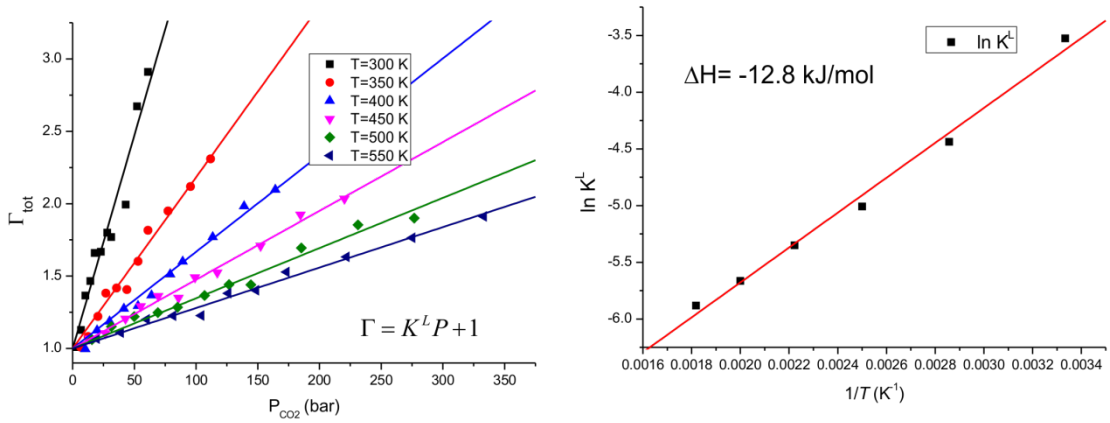

Figure S3. Thermodynamic correction factors for CO_2 adsorbed on a graphite surface as a function of gas pressure at different temperatures (a). The slope of the fitted line is the Langmuir constant (see Appendix, equation A13). (b) The linear fit of the natural logarithm of the Langmuir constant to the inverse temperature, gives the energy of adsorption. The value $-E_{ads}$= ΔH = -12.8 kJ/mol from the slope.

REFERENCES

1. S. García, J. J. Pis, F. Rubiera and C. Pevida, *Langmuir*, 2013, **29**, 6042-6052.
2. C. A. Grande, R. Blom, A. Möller and J. Möllmer, *Chemical Engineering Science*, 2013, **89**, 10-20.
3. M. Sevilla and A. B. Fuertes, *J. Colloid Interface Sci.*, 2012, **366**, 147-154.
4. X. He and M.-B. Hägg, *J. Membr. Sci.*, 2012, **390–391**, 23-31.
5. J. Rouquerol, F. Rouquerol, P. Llewellyn, G. Maurin and K. S. Sing, *Adsorption by powders and porous solids: principles, methodology and applications*, Academic press, 2013.
6. I. Langmuir, *J. Am. Chem. Soc.*, 1918, **40**, 1361-1403.
7. T. S. van Erp, T. T. Trinh, S. Kjelstrup and K. Glavatskiy, *Frontiers in Physics*, 2013, **1**.
8. Y. Jin, D. Lee, S. Lee, W. Moon and S. Jeon, *Analytical Chemistry*, 2011, **83**, 7194-7197.
9. B. B. Saha, S. Jribi, S. Koyama and I. I. E-Sharkawy, *J. Chem. Eng. Data*, 2011, **56**, 1974-1981.
10. X. Shao, Z. Feng, R. Xue, C. Ma, W. Wang, X. Peng and D. Cao, *AIChE J.*, 2011, **57**, 3042-3051.
11. J. Schell, N. Casas, R. Pini and M. Mazzotti, *Adsorption*, 2011, **18**, 49-65.
12. D. Levesque and F. D. Lamari, *Mol. Phys.*, 2009, **107**, 591-597.
13. B. Guo, L. Chang and K. Xie, *Journal of Natural Gas Chemistry*, 2006, **15**, 223-229.
14. S. Himeno, T. Komatsu and S. Fujita, *J. Chem. Eng. Data*, 2005, **50**, 369-376.
15. R. V. Siriwardane, M.-S. Shen, E. P. Fisher and J. A. Poston, *Energy & Fuels*, 2001, **15**, 279-284.
16. M. Heuchel, G. Davies, E. Buss and N. Seaton, *Langmuir*, 1999, **15**, 8695-8705.
17. T. T. Trinh, T. J. Vlugt, M. B. Hagg, D. Bedeaux and S. Kjelstrup, *Front Chem*, 2013, **1**, 38.
18. T. Trinh, T. Vlugt, M. Hägg, D. Bedeaux and S. Kjelstrup, 12th Joint European Thermodynamics Conference, Brescia, July 1-5, 2013 2013.
19. Y. Liu and J. Wilcox, *Environ. Sci. Technol.*, 2012, **47**, 95-101.
20. Z. Xiang, D. Cao, J. Lan, W. Wang and D. P. Broom, *Energy & Environmental Science*, 2010, **3**, 1469-1487.
21. R. Krishna and J. M. van Baten, *J. Membr. Sci.*, 2010, **360**, 323-333.
22. Q. Yang, C. Zhong and J.-F. Chen, *J. Phys. Chem. C*, 2008, **112**, 1562-1569.
23. D. P. Cao and J. Z. Wu, *Carbon*, 2005, **43**, 1364-1370.
24. R. Krishna, *J. Phys. Chem. C*, 2009, **113**, 19756-19781.
25. T. J. H. Vlugt, E. García-Pérez, D. Dubbeldam, S. Ban and S. Calero, *J. Chem. Theory Comput.*, 2008, **4**, 1107-1118.
26. S. K. Schnell, R. Skorpa, D. Bedeaux, S. Kjelstrup, T. J. Vlugt and J.-M. Simon, *J. Chem. Phys.*, 2014, **141**, 144501.
27. O. Talu and I. Zwiebel, *AIChE J.*, 1986, **32**, 1263-1276.
28. F. R. Siperstein and A. L. Myers, *AIChE J.*, 2001, **47**, 1141-1159.
29. A. L. Myers and J. M. Prausnitz, *AIChE J.*, 1965, **11**, 121-127.
30. T. T. Trinh, D. Bedeaux, J. M. Simon and S. Kjelstrup, *Phys. Chem. Chem. Phys.*, 2014, **17**, 1226-1233.
31. T. Trinh, D. Bedeaux, J.-M. Simon and S. Kjelstrup, *Chem. Phys. Lett.*, 2014, **612**, 214.
32. X. He, J. Arvid Lie, E. Sheridan and M.-B. Hägg, *Energy Procedia*, 2009, **1**, 261-268.
33. S. Kjelstrup and D. Bedeaux, *Non-equilibrium thermodynamics of heterogeneous systems*, World Scientific Singapore, 2008.

34. S. K. Schnell, X. Liu, J.-M. Simon, A. Bardow, D. Bedeaux, T. J. H. Vlugt and S. Kjelstrup, *J. Phys. Chem. B*, 2011, **115**, 10911-10918.
35. S. K. Schnell, T. J. H. Vlugt, J.-M. Simon, D. Bedeaux and S. Kjelstrup, *Chem. Phys. Lett.*, 2011, **504**, 199-201.
36. S. K. Schnell, T. J. H. Vlugt, J.-M. Simon, D. Bedeaux and S. Kjelstrup, *Mol. Phys.*, 2011, **110**, 1069-1079.
37. S.-Y. Lee and S.-J. Park, *J. Colloid Interface Sci.*, 2013, **389**, 230-235.
38. Y.-I. Lim, S. K. Bhatia, T. X. Nguyen and D. Nicholson, *J. Membr. Sci.*, 2010, **355**, 186-199.
39. J. Collell and G. Galliero, *J. Chem. Phys.*, 2014, **140**, 194702.
40. M. Szőri and P. Jedlovszky, *J. Phys. Chem. C*, 2014, **118**, 3599-3609.